Environ Sci Pollut Res (2017) 24:13866–13873
DOI 10.1007/s11356-015-5666-1

Traffic aerosol lobar doses deposited in the human respiratory system

Maurizio Manigrasso[1] · **Claudio Vernale**[1] · **Pasquale Avino**[1]

Received: 30 July 2015 / Accepted: 20 October 2015 / Published online: 30 October 2015

Abstract Aerosol pollution in urban environments has been recognized to be responsible for important pathologies of the cardiovascular and respiratory systems. In this perspective, great attention has been addressed to Ultra Fine Particles (UFPs<100 nm), because they efficiently penetrate into the respiratory system and are capable of translocating from the airways into the blood circulation. This paper describes the aerosol regional doses deposited in the human respiratory system in a high-traffic urban area. The aerosol measurements were carried out on a curbside in downtown Rome, on a street characterized by a high density of autovehicular traffic. Aerosol number-size distributions were measured by means of a Fast Mobility Particle Sizer in the range from 5.6 to 560 nm with a 1 s time resolution. Dosimetry estimates were performed with the Multiple-Path Particle Dosimetry model by means of the stochastic lung model. The exposure scenario close to traffic is represented by a sequence of short-term peak exposures: about 6.6×10^{10} particles are deposited hourly into the respiratory system. After 1 h of exposure in proximity of traffic, 1.29×10^{10}, 1.88×10^{10}, and 3.45×10^{10} particles are deposited in the head, tracheobronchial, and alveolar regions. More than 95 % of such doses are represented by UFPs. Finally, according to the greater dose estimated, the right lung lobes are expected to be more susceptible to respiratory pathologies than the left lobes.

Responsible editor: Philippe Garrigues

✉ Maurizio Manigrasso
m.manigrasso@inail.it

[1] DIT, INAIL Research Area, via IV Novembre 144, I-00187 Rome, Italy

Keywords Urban air · Ultrafine particles · Deposition doses · Lung lobes · FMPS · MPPD

Introduction

Aerosol pollution in urban environments has been recognized to be responsible for important pathologies of the cardiovascular (Brook et al. 2002; Simkhovich et al. 2008) and respiratory systems (Delfino et al. 1998; Von Klot et al. 2002), it has also been associated with increased mortality and hospital admissions (Dominici et al. 2006). Directive 2008/50/EC states that for fine particulate matter (PM2.5), there is still no identifiable threshold below which PM2.5 would not pose a risk. Therefore, a general reduction of its concentrations in the urban background should be pursued to ensure that large sections of the population benefit from an improved air quality (Avino et al. 2002, 2004, 2015a; Avino and Manigrasso 2008).

More recently, the International Agency for Research on Cancer (IARC 2015) has considered outdoor pollution as a leading environmental cause of cancer deaths. Furthermore, particulate matter has been classified as carcinogenic to humans (Group 1). Within this context, the importance of aerosol size distribution measurements resides in that the doses deposited in the human respiratory system strictly depend on the particle sizes.

In this perspective, great attention has been addressed to Ultra Fine Particles (UFPs<100 nm) (Donaldson et al. 2001; Oberdörster et al. 2005; Fanizza et al. 2010), since they efficiently penetrate into the respiratory system and are capable of translocating from the airways into the blood circulation (Oberdörster et al. 2005. Moreover, the knowledge of their distribution in the respiratory tree is important because the airway

pathologies caused by deposition of particulate matter have often been reported to occur at specific sites in the lung, particularly within specific lobes (Winkler-Heil and Hofmann 2009). Parkash (1977) observed that the right lung is more often the seat of carcinoma than the left lung, and the upper lobes more often than the lower lobes. The author speculated that since the right bronchus is wider, shorter, and runs almost as a continuation of the trachea, there is a greater chance of more particles being deposited in the right lung than in the left lung as a whole, which is likely to cause a higher frequency of malignancies. For this reason, it is important to assess particle deposition in the respiratory tree, considering the differences between and within the lung lobes. This study relies on time and size-resolved aerosol measurements and focuses on that task by estimating aerosol doses deposited in the lung lobes.

Materials and methods

Aerosol measurements

Aerosol number-size distributions were measured by means of a TSI Fast Mobility Particle Sizer (model 3091, FMPS, Shoreview, MN, USA). The instrument counts and classifies particles, according to their electrical mobility, in 32 size channels, in the range from 5.6 to 560 nm, with a 1 s time resolution. FMPS operates at a high flow rate (10 L min^{-1}) to minimize UFP diffusion losses. It operates at ambient pressure to prevent evaporation of volatile and semivolatile particles (TSI 2009; Manigrasso et al. 2009; Avino et al. 2013a). The performance of the FMPS was investigated by Jeong et al. (2009) by comparison with a Scanning Mobility Particle Sizer (SMPS). The authors evaluated that the SMPS number concentration, in the size range from 6 to 100 nm, is about 34 % lower than the FMPS measurements, due to the diffusion losses of particles in the SMPS. The diffusion loss-corrected SMPS number concentration is on average about 15 % higher than the FMPS data.

Aerosol measurements were carried out on a curbside in downtown Rome. The site (41°53'46" N, 12°29'46" E) is located in an area characterized by a high density of autovehicular traffic, in a narrow double lane street (street width, *W*, of about 8 m), with high buildings on both sides (average height, *H*, of about 25 m). Such a street can be considered as a street canyon, as the aspect ratio *H*/*W* is about 3:1.

An hour of aerosol data collected during the morning traffic peak period has been selected to carry out dosimetry estimates. During such hour, the values of temperature and of relative humidity (average±standard deviation) were 15.9± 0.2 °C and 73±1 %, respectively.

Particle dose evaluation

Particle deposition in the human respiratory system was evaluated using the Multiple-Path Particle Dosimetry Model (MPPD v2.1, ARA 2009), which calculates the deposition and clearance of mono and polydisperse aerosols, from ultrafine to coarse particles in the respiratory system of humans and rats (Anjilvel and Asgharian 1995; Price et al. 2002; Manigrasso et al. 2015a, b). The model includes single and multiple-path methods to calculate airflow and aerosol deposition. Dosimetry estimates were made by means of the stochastic lung model, because it provides a more realistic lung geometry than the symmetric one considered in the ICRP model (ICRP 1994). Symmetric models do not consider the variability of the structural components of the lung. They assume that all airways in the same generation have the same values of diameter length and branching angle. The stochastic lung model takes into account (Koblinger and Hofmann 1985; 1990) the asymmetry of the lung structure and track each inhaled particle through a pathway randomly selected by means of the Monte Carlo method.

In the MPPD model, the ten stochastic lungs proposed by Asgharian et al. (2001) are ordered in a size (total number of airways) from the smallest to the largest and the approximate size percentile of each lung is provided. The 60th percentile human stochastic lung was considered in this study. The following settings were considered in the application of the MPPD model: (i) a uniformly expanding flow, (ii) an upright body orientation, and (iii) nasal breathing with a 0.5 inspiratory fraction and no pause fraction. Moreover, the following parameters were used for a Caucasian adult male under light work physical activity, based on the ICRP report (ICRP 1994): (i) a functional residual capacity (FRC) of 3300 mL, (ii) an upper respiratory tract (URT) volume equal to 50 mL, (iii) a 20 min^{-1} breathing frequency, and (iv) an air volume inhaled during a single breath (tidal volume, V_T) of 1.25 L.

Particle number regional deposition doses in the head (H), trachebronchial (TB), and alveolar (AI) left-upper (LU), left-lower (LL), right-upper (RU), right-middle (RM), and right-lower (RL) lung lobes were calculated as follows:

(i) instant regional doses:

$$D^R(t) = \sum_{i=1}^{32} F_i^R \times C_i(t) \times V_T \quad (1)$$

where t is the time, $F^R{}_i$ is the deposition fraction at a given R region (H, TB, and AI entire lung) of particles classified in the i^{th} size class (calculated by the MPPD model), $C_i(t)$ is the concentration of particles in the i^{th} size class averaged over a single respiratory act time interval. The summation in

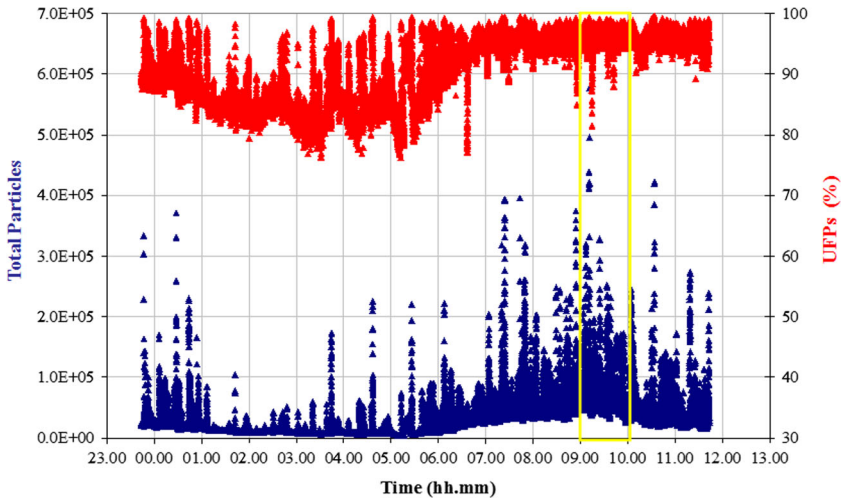

Fig. 1 Temporal trends of total (5.6–560 nm) particle number concentration and of UFP (as %) contribution in a street canyon in downtown Rome

Eq. 1 is carried out over the 32 FMPS size classes.

(ii) one hour regional cumulative doses:

$$D_h^R = \sum_{t=0}^{3600} D^R(t) \quad (2)$$

where R stands for the head (H), tracheobronchial left-lower lobe (TBLL), tracheobronchial right-upper lobe (TBRU), tracheobronchial right-middle lobe (TBRM), tracheobronchial right-lower lobe (TBRL), alveolar left-upper lobe (ALU), alveolar left-lower lobe (ALL), alveolar right-upper lobe (ARU), alveolar right-middle lobe (ARM), and alveolar right-lower lobe (ARL).

The summation in Eq. 2 is carried out over a 1 h (3600 s) time interval divided in 3 s time segments, as the duration of respiratory act.

(iii) cumulative doses deposited at the end of an exposure period ($D^R{}_c$) in head (H), tracheobronchial (TB) and alveolar (AI) regions as function of particle diameter and time. For the TB and AI regions the left-upper (LU), left-lower (LL), right-upper

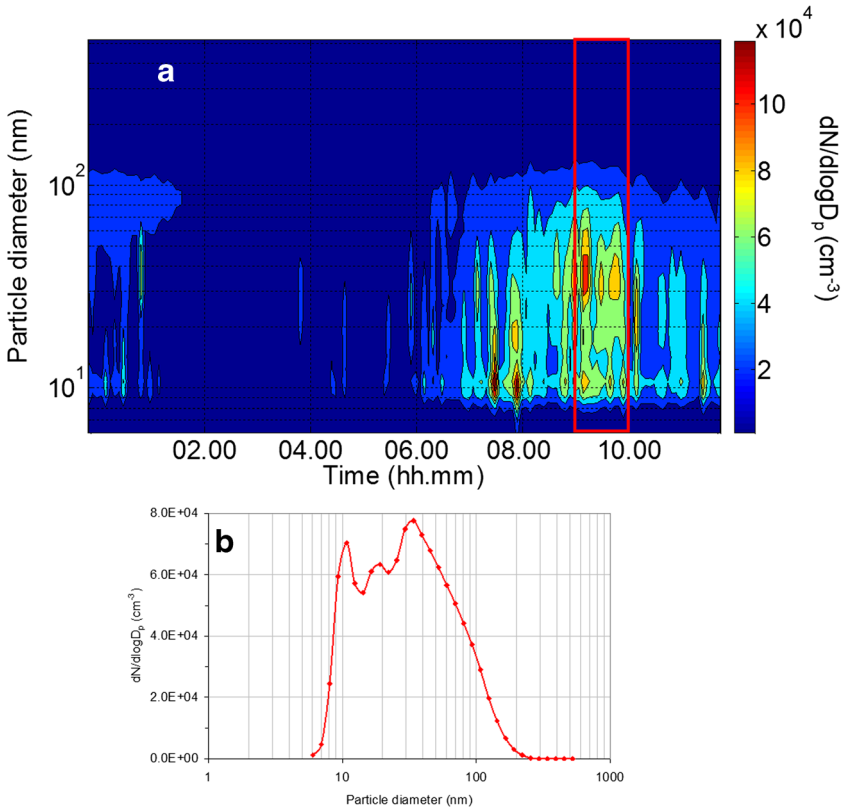

Fig. 2 Temporal variation of aerosol number-size distribution (5 min average of 1 s time resolution data) in a street canyon in downtown Rome throughout a 12 h period (**a**) and mean aerosol number-size distribution (**b**) during the peak traffic hour (the *red box* in figure a)

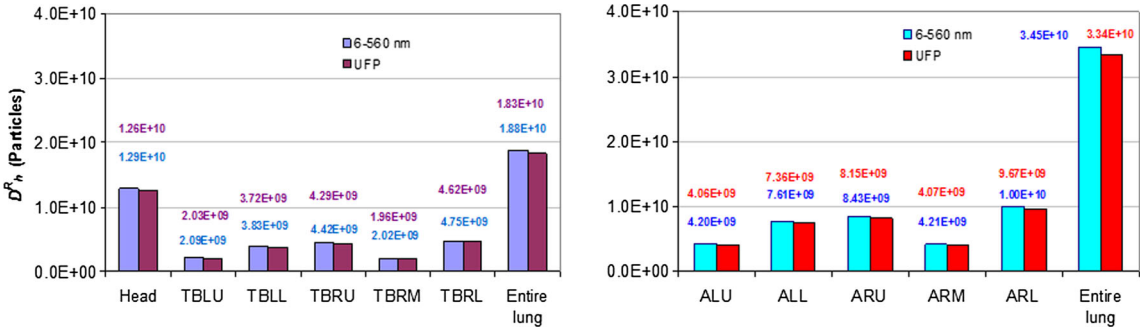

Fig. 3 One hour regional cumulative doses (D^R_h) in the H, TBLU, TBLL, TBRU, TBRM, TBRL, ALU, ALL, ARU, ARM, and ARL regions, after 1 h exposure in traffic proximity. For the acronyms, see text

(RU), right-middle (RM), right-lower (RL) lung lobes were considered.

$$D^R_c = \sum_{t=0}^{t} D^R(t) \quad (3)$$

The summation in Eq. 3 is carried out over variable time intervals ranging from 0 to 3600 s increased by 3 s steps.

Results and discussion

Figure 1 shows the temporal trend of total (5.6–560 nm) particle concentration throughout a 12 h time span together with the percent contribution of UFPs. We selected one-hour size distribution data (the *yellow box* in Fig. 1) to carry out dosimetry estimates. During such time interval, total particle concentration ranged from 2.6×10^4 to 5.8×10^5 particles×cm^{-3}, with an average value of 7.2×10^4 particles×cm^{-3}. The upper limit of such an interval represents the spike concentration due to the instant exhaust emission of auto vehicles passing by the measurement site, whereas the lower limit represents the baseline value for the specific street canyon and time of day considered. In particular, during such 1 h time span, the UFP contribution is on average 95 %, whereas during nocturnal hours (1–4 a.m.) it drops down to 85 %.

Figure 2 describes the temporal evolution of aerosol number-size distribution (5 min averages of 1 s time resolution data) as a function of time throughout the 12 h time period (Fig. 2a) and the average size number-distribution during the 1 h time interval considered for dosimetry estimates (Fig. 2b). In particular, during such period, a trimodal distribution with modes at 10, 19, and 34 nm was observed.

Based on such data, one-hour regional cumulative doses (D^R_h) deposited in the head, tracheobronchial and, alveolar regions are reported in Fig. 3. After 1 h exposure in proximity of traffic 1.29×10^{10}, 1.88×10^{10}, and 3.45×10^{10} particles are deposited in the head, tracheobronchial, and alveolar regions. More than 95 % of such doses are represented by UFPs. Both in tracheobronchial and alveolar regions, doses in RU lobes are about twice as much as those in LU lobes, 24 and 31 % more, respectively, in TBRL than in TBLL and in PRL than in PLL lobes. Compared with the lung lobes, the highest dose was deposited in the H region, about 24 % of the total particle dose.

The relevance of these data resides in that they rely on aerosol measurements carried out in conditions that closely reproduce the real exposure of individuals in proximity of traffic, accounting for the rapid evolution of traffic aerosol. On the contrary, the regulatory approach currently adopted to estimate human exposure to airborne particles is based on the measurement of a 24-hour average mass concentration (PM10, PM2.5) at fixed outdoor monitoring stations (Directive 2008/50/EC; NEPC 1998, 2003; USEPA 2006). Such data are not representative of real outdoor exposure, because particle concentrations, high at the emission point,

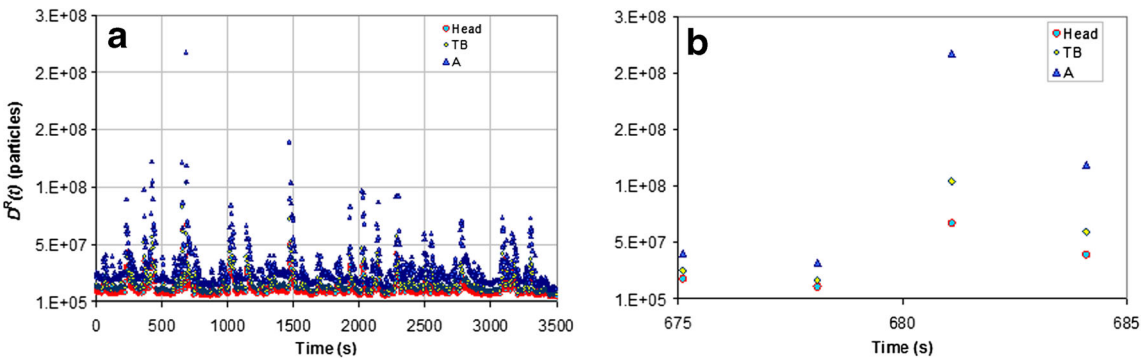

Fig. 4 Instant regional doses ($D^R(t)$) deposited in H, TB, and Al regions as a function of time. Figure **b** is a highlight of Fig. **a**. For the acronyms, see text

rapidly decay with the distance from the source (Marini et al. 2015). Air-quality standards are not defined in terms of number and surface area. Therefore, data from monitoring stations cannot be used to evaluate the doses deposited in the respiratory system. Moreover, short-term dose effects cannot be accounted for by means of average measurements. In fact, close to traffic, the exposure scenario is represented by a sequence of short-term peak exposures.

Such issue is addressed by Fig. 4a, where instant regional doses ($D^R(t)$) deposited in the head, tracheobronchial, and alveolar regions are reported as a function of time throughout the same time interval considered to estimate the cumulative doses (D^R_h, Fig. 3). In this graphic, each data point represents the total particle number deposited after a tidal volume inhalation. In proximity to traffic, within a single respiratory act, the particle dose deposited in the H, TB, and AI regions may increase by about 500 % as shown in Fig. 4b.

In the contour plots of Figs. 5, 6, and 7, the cumulative doses of particle deposited (D^R_c) are reported as a function of time and particle diameter for the head region and the five lung lobes both in the tracheobronchial and in the alveolar regions, respectively.

At the end of the 1 h exposure period, the size distributions of particle-deposited doses follow a trimodal distribution with modes at 10, 16, and 29 nm for the H and TB region and 10, 19, and 29 nm for the alveolar region. Deposited in the H region are 1.5×10^9, 8.9×10^8, and 7.0×10^8 particles, respectively for 10, 19, and 29 nm particle diameters. At modal diameters, the particle-deposited doses are in the range of 2.1×10^8–5.0×10^8, 1.4×10^8–3.3×10^8, and 1.2×10^8–2.7×10^8, respectively for the TB region and 2.8×10^8–6.9×10^8, 3.0×10^8–7.0×10^8, and 3.2×10^8–8.0×10^8, respectively for the Al region.

It is worth observing that the mode at 10 nm represents the main contribution to the cumulative dose deposited in H and

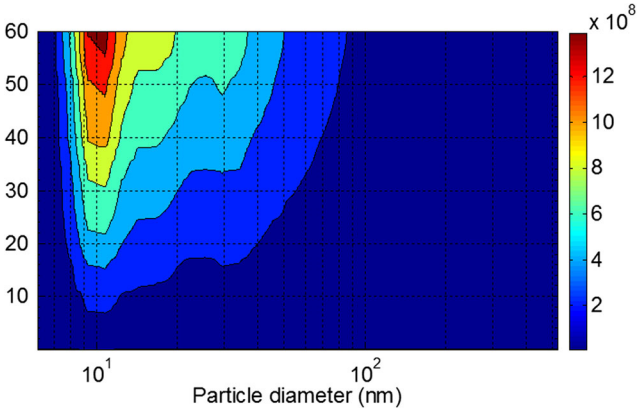

Fig. 5 Cumulative dose (D^R_c) for H region, as a function of time and particle diameter

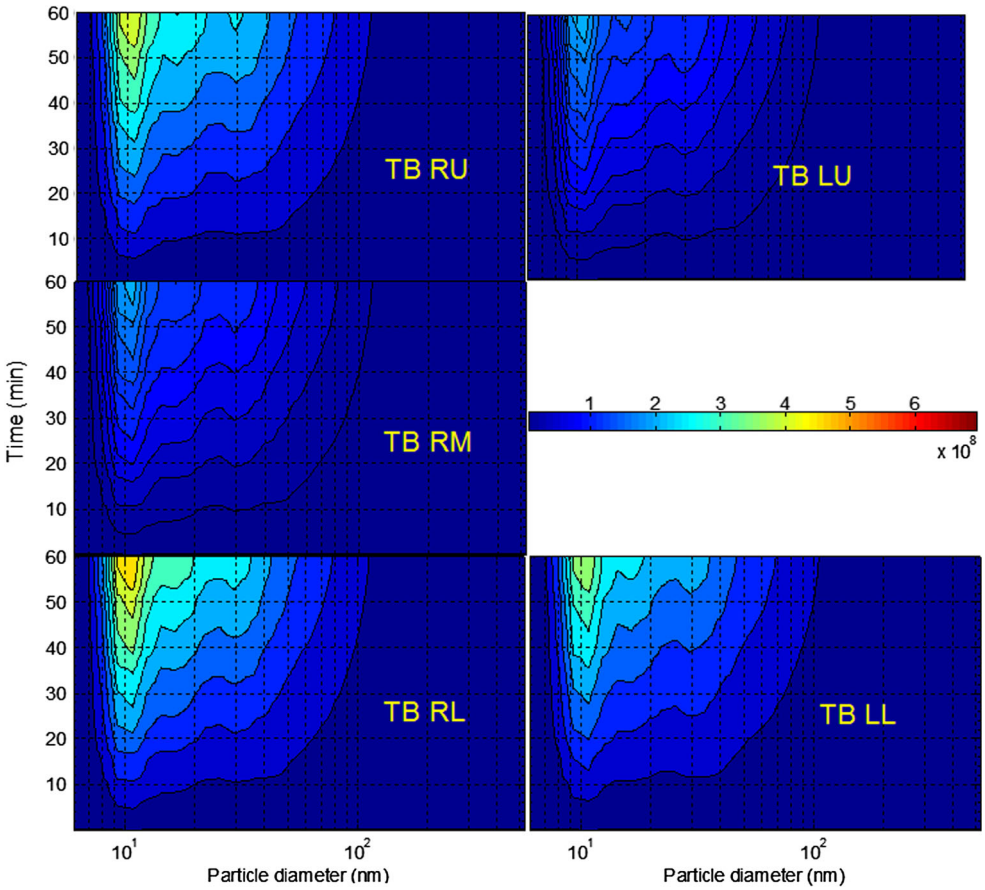

Fig. 6 Cumulative dose (D^R_c) for lung lobes in TB region, as a function of time and particle diameter

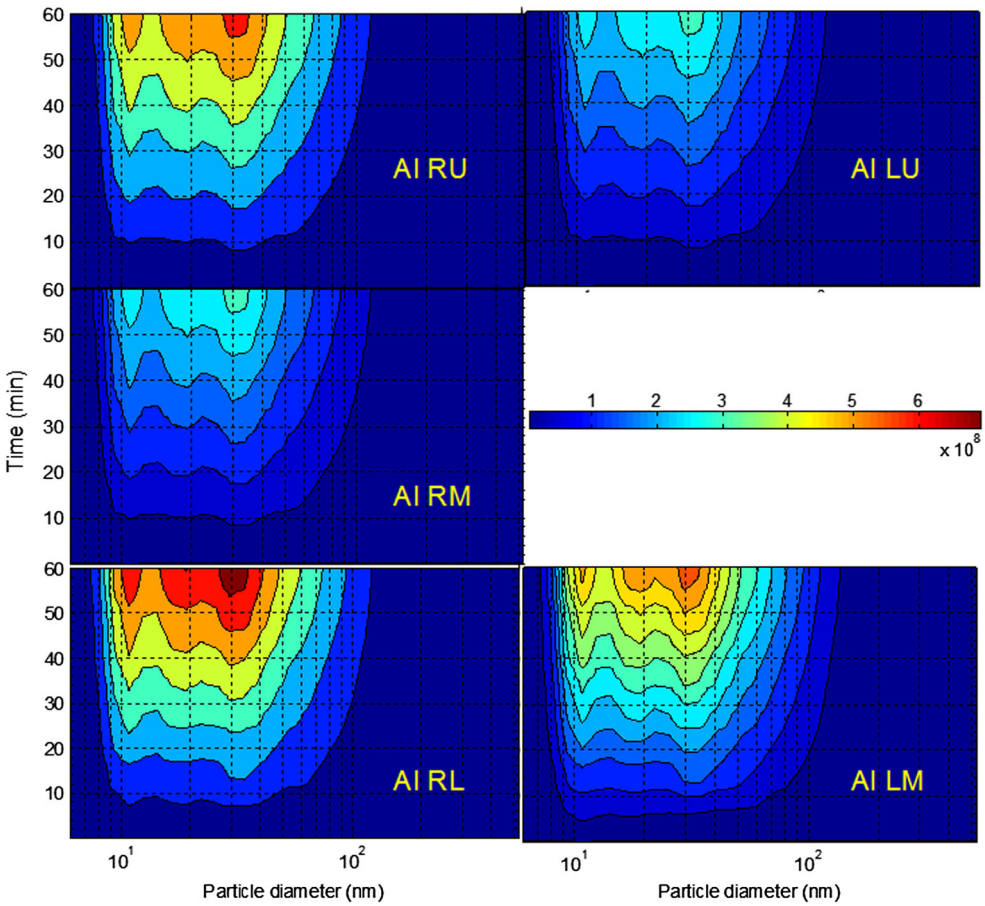

Fig. 7 Cumulative dose (D^R_c) for lung lobes in AI region, as a function of time and particle diameter

TB regions (Figs. 5 and 6), whereas for the AI region, the greater contribution is due to the mode at 29 nm (Fig. 7). In particular, for the daytime and traffic site considered, about 28 % of the particles below 10 nm are deposited in the head region. These particles are formed by the nucleation of semivolatile organic compounds in vehicle exhaust. Their persistence in the atmosphere is relatively low with respect to larger-sized particles. Then, they are predominant during the day when freshly formed and decrease significantly at night when traffic is less intense (Manigrasso and Avino 2012). They are responsible for the high frequency contribution observable in the temporal trend of total particle concentration (Fig. 1) (Avino et al. 2011, 2013b, 2015b; Manigrasso et al. 2013).

From the health point of view, UFPs may translocate from the blood circulation to other organs such as the liver, spleen, kidneys, heart, and brain (Peters et al. 2006). Indeed, the health relevance of the high UFP dose estimated for the head region (Fig. 3), in particular for the small-size fraction below 10 nm (Fig. 5) is linked to its ability to reach to brain. The central nervous system can be targeted by airborne UFPs. The most likely mechanism is from deposits on the olfactory mucosa of the nasopharyngeal region of the respiratory tract and subsequent translocation via the olfactory nerve (Oberdörster et al. 2004). Particles, on entering the brain, may possibly entail neurodegenerative consequences. Histological evidence of neurodegeneration has been reported in both canine and human brains exposed to high ambient PM levels, suggesting the potential for neurotoxic consequences (Terzano et al. 2010).

Conclusions

Aerosol number-size distributions were measured with 1 s time resolution, on a curbside in a street canyon. Based on these, the aerosol doses deposited in the respiratory system were estimated for individuals exposed in proximity of traffic. During peak traffic hours, after 1 h exposure about 6.6×10^{10} particles were deposited into the respiratory system. Such dose was almost entirely made of UFPs and was asymmetrically deposited into the lung lobes: more in the right than in the left lung lobes. According to the greater dose estimated, the right lung lobes are expected to be more susceptible to respiratory pathologies than the left lobes. The cumulative doses deposited into the respiratory system followed a trimodal distribution with modes between 10 and 29 nm. For deposited particles below 10 nm, the highest dose was estimated for the head region, where from the olfactory mucosa they may possibly translocate to brain.

Acknowledgments The authors wish to thank ARA for MPPD version 2.1.

This study was supported by INAIL grants P19L08, P20L01 and P20L09.

References

Anjilvel S, Asgharian BA (1995) Multiple-path model of particle deposition in the rat lung. Fundam Appl Toxicol 28:41–50

Applied Research Associates (ARA) 2009 Multiple-Path Particle Dosimetry Model (MPPD v 2.11). http://www.ara.com

Asgharian B, Hofmann W, Bergmann R (2001) Particle deposition in a multiple-path model of the human lung. Aerosol Sci Technol 34: 332–339

Avino P, Manigrasso M (2008) Ten-year measurements of gaseous pollutants in urban air by an open-path analyzer. Atmos Environ 42: 4138–4148

Avino P, Brocco D, Cecinato A, Lepore L, Balducci C (2002) Carbonaceous components in atmospheric aerosol: measurement procedures and characterization. Ann Chim 92:333–341

Avino P, De Lisio V, Grassi M, Lucchetta MC, Messina B, Monaco G, Petraccia L, Quartieri G, Rosentzwig R, Russo MV, Spada S, Valenzi VI (2004) Influence of air pollution on chronic obstructive respiratory diseases: comparison between city (Rome) and hillcountry environments and climates. Ann Chim 94:629–636

Avino P, Casciardi S, Fanizza C, Manigrasso M (2011) Deep investigation of ultrafine particles in urban air. Aerosol Air Qual Res 11:654–663

Avino P, Manigrasso M, Fanizza C, Carrai P, Solfanelli L (2013a) Submicron particles in smoke resulting from welding alloys and cast alloy in metalworking industry. Med Lav 104:335–350

Avino P, Lopez F, Manigrasso M (2013b) Regional deposition in human respiratory system of submicrometer aerosol determined at 1 Hz frequency. Aerosol Air Qual Res 13:1702–1711

Avino P, Manigrasso M, Rosada A, Dodaro A (2015a) Measurement of organic and elemental carbon in downtown Rome and background area: physical behavior and chemical speciation. Environ Sci Process Impacts 17:300–315

Avino P, Manigrasso M, Pandolfi P, Tornese C, Settimi D, Paolucci N (2015b) Submicron particles during macro-and micro-weldings procedures in industrial indoor environments and health implications for welding operators. Metals 5:1045–1060

Brook RD, Brook JR, Urch B, Vincent R, Rajagopalan S, Silverman F (2002) Inhalation of fine particulate air pollution and ozone causes acute arterial vasoconstriction in healthy adults. Circulation 105: 1534–1536

Delfino RJ, Zeiger RS, Seltzer JM, Street DH (1998) Symptoms in pediatric asthmatics and air pollution: differences in effects by symptom severity, anti-inflammatory medication use and particulate averaging time. Environ Health Perspect 106:751–761

Directive 2008/50/EC of the European Parliament and of the Council of 21 May 2008 on ambient air quality and cleaner air for Europe. Official Journal of the European Union. L 152 11 June 2008.

Dominici F, Peng RD, Bell ML, Pham L, McDermott A, Zeger SL, Samet JM (2006) Fine particulate air pollution and hospital admission for cardiovascular and respiratory diseases. JAMA, J Am Med Assoc 295:1127–1134

Donaldson K, Stone V, Seaton A, MacNee W (2001) Ambient particle inhalation and the cardiovascular system: potential mechanisms. Environ Health Perspect 109:523–527

Fanizza C, Casciardi S, Avino P, Manigrasso M (2010) Measurements and characterization by transmission electron microscopy of ultrafine particles in the urban air of Rome. Fresenius Environ Bull 19:2026–2032

IARC (2015) Monographs on the evaluation of carcinogenic risks to humans: outdoor air pollution. International Agency for Research on Cancer, Lyon

ICRP (1994) Human respiratory tract model for radiological protection. A report of a task group of the International Commission on Radiological Protection. Ann ICRP 24:1–482

Jeong C-H, Greg J, Evans GJ (2009) Inter-comparison of a fast mobility particle sizer and a scanning mobility particle sizer incorporating an ultrafine water-based condensation particle counter. Aerosol Sci Technol 43:364–373

Koblinger L, Hofmann W (1985) Analysis of human lung morphometric data for stochastic aerosol deposition calculations. Phys Med Biol 30:541–556

Koblinger L, Hofmann W (1990) Monte Carlo modeling of aerosol deposition in human lungs. Part I: simulation of particle transport in stochastic lung structure. J Aerosol Sci 21:661–674

Manigrasso M, Avino P (2012) Fast evolution of urban ultrafine particles: implications for deposition doses in the human respiratory system. Atmos Environ 51:116–123

Manigrasso M, Avino P, Fanizza C (2009) Ultrafine particles in the urban area of Rome. Fresenius Environ Bull 18:1341–1347

Manigrasso M, Stabile L, Avino P, Buonanno G (2013) Influence of measurement frequency on the evaluation of short-term dose of sub-micrometric particles during indoor and outdoor generation events. Atmos Environ 67:130–142

Manigrasso M, Buonanno G, Fuoco FC, Stabile L, Avino P (2015a) Aerosol deposition doses in the human respiratory tree of electronic cigarette smokers. Environ Pollut 196:257–267

Manigrasso M, Buonanno G, Stabile L, Morawska L, Avino P (2015b) Particle doses in the pulmonary lobes of electronic and conventional cigarette users. Environ Pollut 202:24–31

Marini S, Buonanno G, Stabile L, Avino P (2015) A benchmark for numerical scheme validation of airborne particle exposure in street canyons. Environ Sci Pollut Res 22:2051–2063

NEPC (1998) National environment protection measure and impact statement for ambient air quality. National Environment Protection Council, Adelaide

NEPC (2003) Variation to the national environment protection (ambient air quality) measure. National Environment Protection Council, Adelaide

Oberdörster G, Sharp Z, Atudorei V, Elder A, Gelein R, Kreyling W, Cox C (2004) Translocation of inhaled ultrafine particles to the brain. Inhal Toxicol 16:437–445

Oberdörster G, Oberdörster E, Oberdörster J (2005) Nanotoxicology: an emerging discipline evolving from studies of ultrafine particles. Environ Health Perspect 113:823–840

Parkash O (1977) Lung cancer. A statistical study based on autopsy data from 1928 to 1972. Respiration 34:295–304

Peters A, Veronesi B, Calderón-Garcidueñas L, Gehr P, Chen LC, Geiser M, Reed W, Rothenrutishauser B, Schürch S, Schulz H (2006) Translocation and potential neurological effects of fine and ultrafine particles a critical update. Part Fibre Toxicol 3:13. doi:10.1186/1743-8977-3-13

Price OT, Asgharian B, Miller FJ, Cassee FR, de Winter-Sorkina R (2002) Multiple Path Particle Dosimetry Model (MPPD v. 1.0): a model for human and rat airway particle dosimetry, v 1.0. National Institute for Public Health and the Environment (RIVM), Bilthoven, The Netherlands. http://www.ara.com/products/mppd.htm. Accessed 21 July 2015.

Simkhovich BZ, Kleinman MT, Kloner RA (2008) Air pollution and cardiovascular injury epidemiology, toxicology, and mechanisms. J Am Coll Cardiol 52:719–726

Terzano C, Di Stefano F, Conti V, Graziani E, Petroianni A (2010) Air pollution ultrafine particles: toxicity beyond the lung. Eur Rev Med Pharmacol Sci 14:809–821

TSI (2009) www.tsi.com/uploadedFiles/Product_Information/Literature/Catalogs/Particle_Catalog_ Web.pdf. Accessed 21 July 2015.

USEPA (2006) U.S. Environmental Protection Agency 40 CFR Part 50, 2006. In: National Ambient Air Quality Standards for Particulate Matter, Part II. Final Rule

Von Klot S, Wölke G, Tuch T, Heinrich J, Dockery DW, Schwartz J, Kreylingz WG, Wichmann HE, Peters A (2002) Increased asthma medication use in association with ambient fine and ultrafine particles. Eur Respir J 20:691–702

Winkler-Heil R, Hofmann W (2009) Inter- and intra-lobar deposition of inhaled particles. Proc. Eur Aerosol Conf 2009, Karlsruhe, Abstract T101A01.